Identification and Compensation of Force Ripple in Linear Permanent Magnet Motors

Christof Röhrig and Andreas Jochheim
Department of Electrical Engineering
University of Hagen
D-58084 Hagen, Germany
christof.roehrig@fernuni-hagen.de

Abstract

The main problem in improving the tracking performance of linear permanent magnet motors is the presence of force ripple caused by the irregular magnetic field of the permanent magnets and inaccuracy in electronic commutation by the servo amplifier. This paper presents a method to identify and compensate the effect of the force ripple in servo control. A physical model of the linear motor and the force ripple is derived first. The identification of the model parameters is done in a closed position control loop by measurement of the control signal for movements with different load forces. No additional sensors (e.g. force sensors) are necessary. A comparison of the tracking performance with and without ripple compensation is given.

1 Introduction

Linear motors are beginning to find widespread industrial applications, particularly for tasks requiring a high precision in positioning such as various semiconductor fabrication and inspection processes [1]. If available, high precision steel cutting machines would save grinding and honing processing which are necessary today [2]. Other possible applications are high speed milling and laser cutting. The main benefits of linear motors are the high force density achievable and the high positioning precision and accuracy associated with the mechanical simplicity of such systems. The electromagnetic force is applied directly to the payload without any mechanical transmission such as chains or screw couplings. This greatly reduces nonlinearities and disturbances caused by backlash and additional frictional forces [3]. The traditional indirect drive design for high speed machine tools, which consists of a rotary motor with a ball-screw transmission to the slide, is limited in speed, acceleration, and accuracy. A linear motor has no mechanical limitations of acceleration and velocity. The velocity is only limited by power electronics or by the bandwidth of the position measurement system. The more predominant nonlinear effects underlying a linear motor system are friction and force ripples arising from imperfections in the underlying components e.g. irregular magnetic field, inaccuracy of commutation. To avoid force ripple different methods have been published. The arrangement of the permanent magnets can be optimized to reduce cogging forces [4],[5]. In [6] a force ripple model is developed and identification is carried out with a force sensor and a frictionless air bearing support of the motor carriage. In [7] a neuronal-network based feedforward controller is proposed to reduce the effect of force ripple. Position-triggered repetitive control is presented in [8]. Other approaches are based on disturbance observers [9], [10], iterative learning control [11] or adaptive control [12]. In this paper a model based approach is proposed, because force ripple is a highly reproducible and time-invariant disturbance. The force ripple model is based on a Fourier series approximation and is identified by measuring the control signal in a closed position control loop for different load forces. The model considers both, current-dependent and current-independent force ripple. The paper is organized as follows: In Section 2 the experimental setup is described. In Section 3, a physical model of the linear motor is derived and explained. The identification of the model parameters are presented. In Section 4 the force ripple compensation is presented and a comparison of the tracking performance with and without ripple compensation is given. Finally Section 5 concludes the paper.

2 Experimental Setup

2.1 Linear Motor

The motors considered here are brushless permanent magnet linear motors with epoxy cores. A linear motor consists on a stator and a moving translator (counterpart of the rotor in a rotating motor). There are two basic classifications of permanent magnet servo motors: epoxy core (i.e. non-ferrous, slotless) and steel core. Epoxy core motors have coils wound within epoxy support. This motors have a closed magnetic path through the gap since two magnetic plates ”sandwich” the coil assembly. The stator induces a multipole magnetic field in the air gap between the magnetic plates. The magnet assembly consists of rare earth magnets, mounted in alternate

polarity on the steel plates. The electromagnetic thrust force is produced by the interaction between the permanent magnetic field in the stator and the magnetic field in the translator driven by the current of the servo amplifier. The linear motors under evaluation are current-controlled three-phase motors driving carriages supported by roller bearings. The commutation of the three phases is done electronically in the power amplifier with the help of a sinusoidal analog hall sensor. Figure 1 shows the unmounted translator with hall sensor and the stator of a linear motor. In the experimental setup two different linear motors (LEA-S-4-S and LEM-S-4-S) are used.

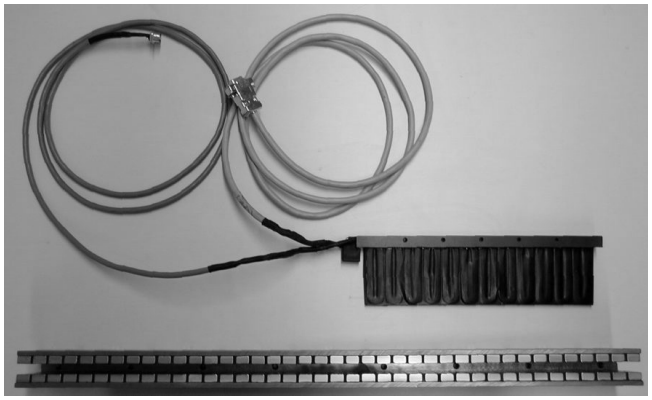

Figure 1: Brushless linear motor LEA-S-4-S (Anorad Inc.)

2.2 Servo Amplifier

The servo amplifier used in the setup is a PWM type with closed current control loop. The servo amplifier uses sinusoidal commutation. The sinusoidal commutation is done with the help of an analog hall sensor. The servo amplifier is manufactured by Custom Servo Motors (CSM, Germany). Figure 2 shows the block structure of the CSM servo amplifier.

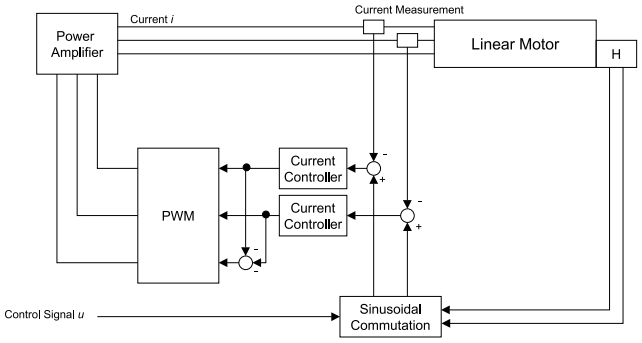

Figure 2: Block diagram of CSM servo amplifier TBF [13]

The maximum input signal of the servo amplifier ($\pm 10V$) correlates to the adjustable peak current of the current loop. In the setup the peak current is adjusted to $10A$. The PWM works with a switching frequency of $9.5kHz$. The current loop bandwidth is specified with $1kHz$. The dynamics of the servo amplifier will not be considered as they play a minor role in the dynamics of the whole system.

3 System Analysis and Modeling

Two types of position dependent disturbances are considered: cogging force and force ripple. Cogging is a magnetic disturbance force that is caused by attraction between permanent magnets and translator. The force depends on the relative position of the translator with respect to the magnets, and it is independent of the motor current. Force ripple is an electromagnetic effect and causes a periodic variation of the force constant c_ϕ. Force ripple occurs only if the motor current is different from zero, and its absolute value depends on the required thrust force and the relative position of the translator to the stator. Both disturbances are periodic functions of the position. [8]

Cogging is negligible in motors with iron-less translators [14]. Figure 3 shows the nonlinear block diagram of a servo system with brushless linear motor. The nonlinear disturbances are the velocity depended friction force $F_{friction}$, and the position dependent cogging force $F_{cogging}$ and force ripple $c_\phi(x)$.

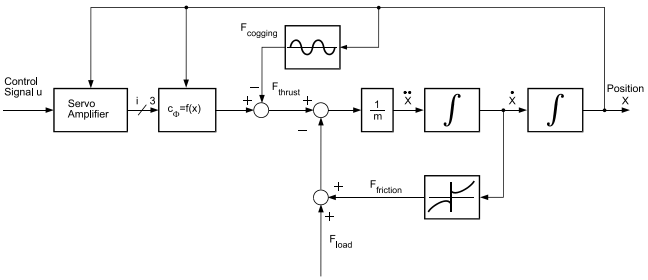

Figure 3: Nonlinear model of a brushless linear motor

The friction force is modeled with a kinetic friction model. In the kinetic friction model the friction force is a function of velocity only. The friction curve is identified with experiments at different velocities. The friction has a discontinuity at $\dot{x} = 0$, because of stiction. Stiction avoid accurate measurement of the thrust force without motion of the carriage. A survey of friction models and compensation methods is given in [15]. Advanced friction modeling, identification and compensation can be found in [16].

Aim of the force ripple identification is to obtain a function of the thrust force F_{thrust} versus the control signal u and the position x.

$$F_{thrust} = f\left(u, x\right) \tag{1}$$

A possible solution to identify this function is to measure the thrust force F_{thrust} at different positions x and control signals u. In this case an additional force sensor and a screw cylinder for manual position adjustment is necessary. To measure the force ripple accurately, without motion of the carriage, a frictionless air bearing support is necessary [6]. A solution to avoid frictionless air bearings is the measurement of the thrust force with moving carriage. At constant velocities the friction force is also constant and can be treated as additional load force. In this case an additional servo system is needed to achieve the movement [17].

The main idea of the proposed identification method is to identify the force ripple in a closed position control loop by measuring the control signal u at different load forces F_{load} and positions x. Neither additional force sensor nor device for position adjustment are necessary. In order to avoid inaccuracy by stiction the measurement is achieved with moving carriage. The position of the carriage is obtained from an incremental linear optical encoder with a measurement resolution of $0.1\mu m$. The experiment consists of several movements at constant low velocity ($1mm/s$) and different load forces ($0 \ldots 70N$). The output of the position controller is stored at equidistant positions. A controller with an integral component is used to eliminate steady position error. During motion with constant low velocity the dynamics of the motor have no significant effect on the control signal u. Figure 4 shows one experimental setup with load forces achieved with pulleys and weights. In another setup the motor is mounted vertically. In this case no pulleys are required, the load force is achieved directly with additional weights attached to the carriage.

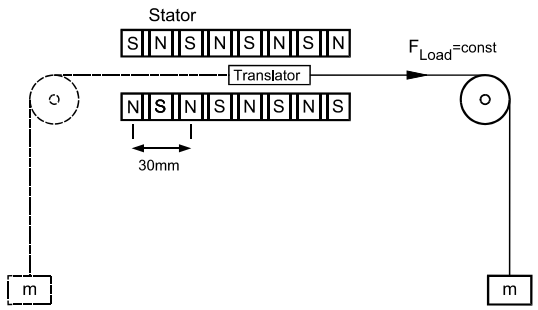

Figure 4: Experiment to load the translator with different forces

Figure 5 shows the controller output u versus the translator position x. In this first experiment there is no additional load force attached to the carriage. The period spectrum of the controller signal u_i is carried out via FFT.

$$u_i = f\left(x_i\right) = \frac{1}{N}\sum_{k=0}^{N-1} c_k \mathrm{e}^{j2\pi k\frac{x_i}{L}} \tag{2}$$

$$x_i = x_0 + i\frac{L}{N}, i = 0 \ldots N-1 \tag{3}$$

$$c_k = \sum_{i=0}^{N-1} u_i \mathrm{e}^{-j2\pi k\frac{x_i}{L}} \tag{4}$$

Where L is the length of the movement, N is the number of measured signals and c_k are the complex discrete Fourier coefficients.

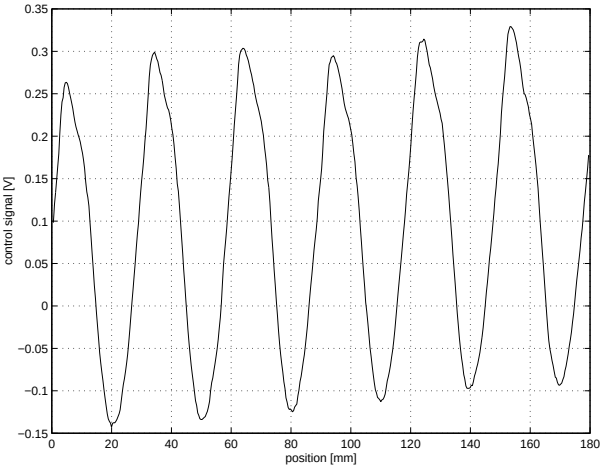

Figure 5: Force ripple without additional load force

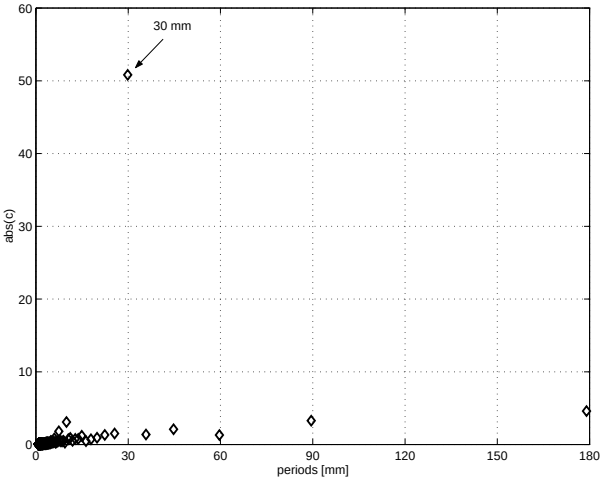

Figure 6: Spectrum of force ripple without additional load force

Figures 6 and 8 display absolute values of the Fourier coefficients $|c_k|$ as rhombuses versus corresponding discrete peri-

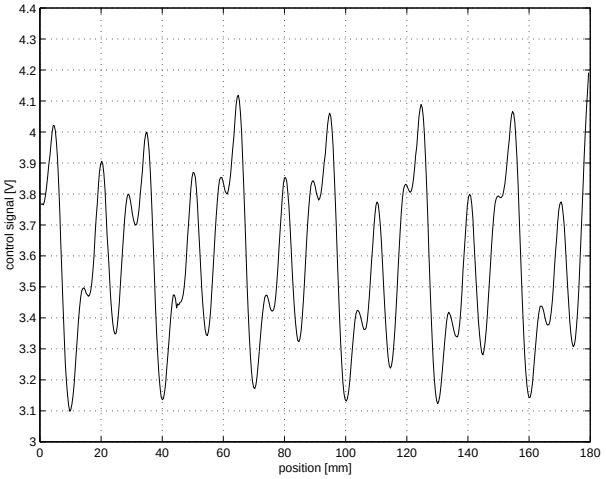

Figure 7: Force ripple at load force F = 70 N

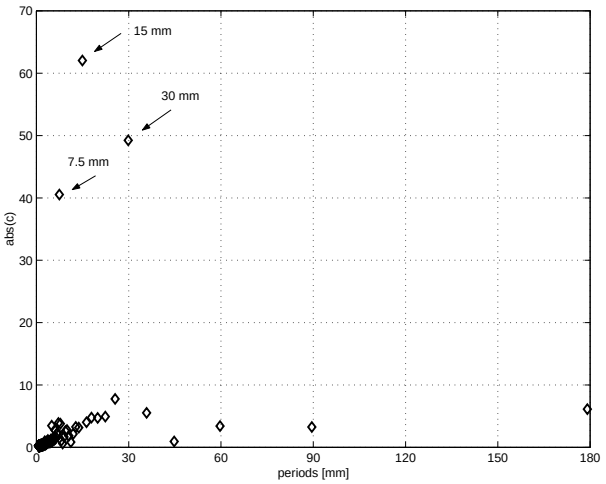

Figure 8: Spectrum of force ripple at load force F = 70 N

ods L/k. Figure 6 shows the period spectrum of the experiment without additional load force. The fundamental period ($30mm$) correspondents to the distance between two permanent magnets with the same polarity in the stator. Figure 7 displays the controller signal with an additional load force of $70N$. The spectrum in figure 8 indicates two additional harmonics at $15mm$ and $7.5mm$. The sinusoid with the period of $30mm$ appears at the same level as the experiment without additional load force. This current-independent ripple is measured even though the translator is build without iron. At heavy load forces the current-dependent force ripple prevails the current-independent ripple. Force ripple can be modeled as a sinusoid with higher order harmonics. The force ripple is complex in shape e.g., due to variations in the magnetic field of the stator. It is a periodic function and can be approximated with a Fourier series. The numerical analysis of the measured data was done with MATLAB^{TM}. The discrete Fourier Transformation has the disadvantage that only periods for whole-numbered divisors of the measured movement can be detected. In order to determine the period more exactly, the data-fitting optimization of MATLAB^{TM} was applied on function (5).

$$f(x) = c_1 + c_2 x + \sum_{k=0}^{M-1} c_{2k+4} \sin\left(\frac{2\pi\,(k+1)}{c_3}\,(x + c_{2k+5})\right) \tag{5}$$

The physical meaning of the parameter vector **c** of function (5) is: c_1 is the average of the controller signal (desired thrust force), c_2 is the gradient of the curve e.g. caused by sealing bellows, c_3 is the highest dominant period, c_{2k+4} are the amplitudes of the sinusoids, c_{2k+5} are the phase shifts of the sinusoids and M is the number of detected sinusoids with spectrum analysis.

The minimization (6) is done with the N measured controller signals u_i at positions x_i. The result of the minimization is a parameter vector **c** of model function (5) that best fits the measured curve.

$$\min_c \sum_{i=0}^{N} \left(f(x_i, c) - u_i\right)^2 \tag{6}$$

The nonlinear least square algorithm of MATLAB^{TM} uses the "large-scale algorithm" based on the "interior-reflective Newton method" for optimization of the vector **c** [18]. The initial values of **c** are taken from the previous spectrum analyses. An identification procedure was written in the MATLAB^{TM} scripting language. The procedure does the optimization of **c** with data of experiments at different load forces. It detects whether the amplitudes c_{2k+4} depend on the load force ($\sim c_1$) or not. The result of the identification procedure are the parameters of function (7) for linearization of function (1) to compensate the effect of the force ripple.

$$u(x, u') = \alpha(x) + \beta(x)\,u' \tag{7}$$

$$\alpha(x) = k_c x + \sum_{k=1}^{M} a_k \sin\left(\frac{2\pi k}{\lambda_0}\,(x + c_k)\right) \tag{8}$$

$$\beta(x) = 1 + \sum_{k=1}^{N} b_k \sin\left(\frac{2\pi k}{\lambda_1}\,(x + d_k)\right) \tag{9}$$

Where M is the number of current-independent sinusoids, N is the number of current-dependent sinusoids, x is the position of carriage, u' is the controller output (desired thrust

force), u is the servo amplifier input, k_c is the gradient of the curve e.g. caused by sealing bellows, a_k are the current-independent amplitudes, b_k are the current-dependent amplitudes, c_k, d_k are the phase shifts and λ_0, λ_1 are the periods. Table 1 shows the identified force ripple parameters of both Anorad linear motors.

In Figure 9 a comparison of the model and the measured control signal is shown. The carriage was loaded with a negative force. The differences between the curves are caused by inaccuracies of position and dimension for individual magnets. The model assumes perfect periodicity of the ripple force.

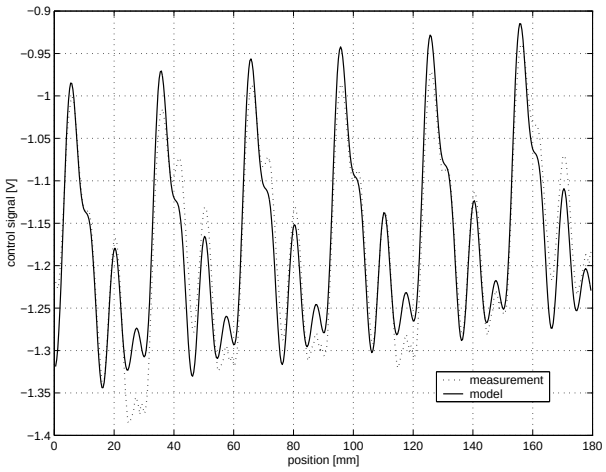

Figure 9: Comparison of model and measurement

4 Force Ripple Compensation

Figure 10 shows the block diagram of the servo control system. To achieve a better tracking performance, a feedforward controller is applied. Feedback control without feedforward control always introduces a phase lag in the command response. Feedforward control sends an additional output, besides the feedback output, to drive the servo amplifier input to desired thrust force. The feedforward control compensates the effect of the carriage mass and the friction force. The friction force is modeled by a kinetic friction model and identified with experiments at different velocities. The mass of the carriage is identified with a dynamic least square algorithm. The stability of the system is determined by the feedback loop. Feedback linearization of friction with the kinetic friction model has been proposed in numerous literature references, but is rarely applied successfully because undesirable oscillations result easily from this approach [16]. The compensation of the force ripple is applied with input-output linearization. The function $\beta(x)$ compensates the effect of the current-dependent ripple the function $\alpha(x)$ the effect of current-independent ripple. Figure 11 compares the tracking error of a movement without ripple compensation with the

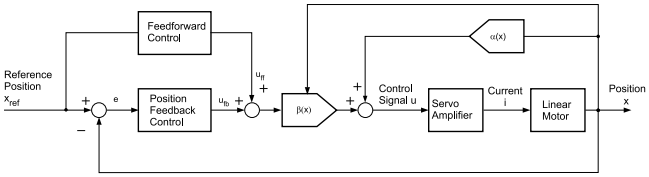

Figure 10: Force ripple compensation

movement with ripple compensation. In this measurement, the carriage moves from position $50mm$ to position $150mm$ and back to position $50mm$ with $v_{max} = 200mm/s$. If the ripple compensation is applied, the tracking error is reduced significantly. Figure 12 shows the control signal u and the output of the feedforward controller with force ripple compensation. The difference between the signals are caused by model inaccuracies.

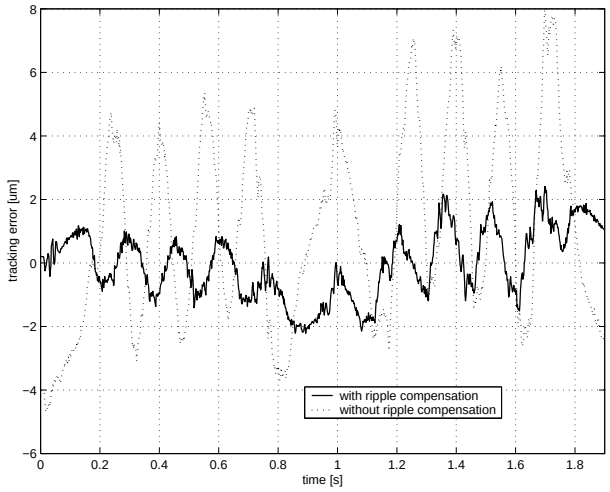

Figure 11: Tracking error

5 Conclusion

In this paper, a model-based force ripple identification and compensation is presented. The force ripple model is based on Fourier series approximation of the periodic ripple function. To identify the model parameters, no additional sensors are required. The necessary additional load force is attached by pulleys and weights. The model was identified with non-iron-coil permanent magnet motors. Since it considers current-independent ripple, it can also be applied on iron-coil permanent magnet motors. Experiments show that the tracking performance is significantly improved if the ripple compensation is applied. In further investigations, the necessary load force will be attached by acceleration of the carriage.

Table 1: Identified force ripple parameters

Motor	N	M	k_c	λ_0/mm	a_1	c_1/mm	λ_1/mm	b_1	b_2	d_1/mm	d_2/mm
LEA-S-4-S	2	1	0.00036	30.0	0.11	0.0	15.0	0.071	0.045	4.7	0.6
LEM-S-4-S	2	0	-0.0020	-	-	-	14.7	0.14	-0.049	1.8	2.5

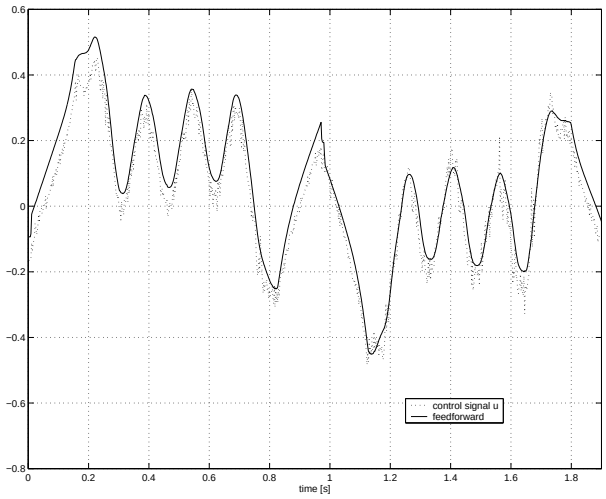

Figure 12: Controller Signals

References

[1] A. Basak, *Permanent-Magnet DC Linear Motors*, Clarendon Press, Oxford, 1996.

[2] G. Brandenburg, S. Brückel, J. Dormann, J. Heinzl, and C. Schmidt, "Comparative Investigation of Rotary and Linear Motor Feed Drive System for High Precision Machine Tools," in *Proceedings of the 6th International Workshop on Advanced Motion Control*, Nagoya, Japan, Apr. 2000, pp. 384–389.

[3] G. Pritschow, "A Comparison of Linear and Conventional Electromechanical Drives," *Annals of the CIRP*, vol. 47, no. 2, pp. 541–548, 1998.

[4] I.S. Jung, J. Hur, and D.S. Hyun, "3-D Analysis of Permanent Magnet Linear Synchronous Motor with Magnet Arrangement Using Equivalent Magnetic Circuit Network Method," *IEEE Transactions on Magnetics*, vol. 35, no. 5, pp. 3736–3738, Sept. 1999.

[5] T. Yoshimura, H.J. Kim, M. Watada, S. Torij, and D. Ebihara, "Analysis of the Reduction of Detent Force in a Permanent Magnet Linear Synchronous Motor," *IEEE Transactions on Magnetics*, vol. 31, no. 6, pp. 3728–3730, Sept. 1995.

[6] P. Van den Braembussche, J. Swevers, H. Van Brussel, and P. Vanherck, "Accurate Tracking Control of Linear Synchronous Motor Machine Tool Axes," *Mechatronics*, vol. 6, no. 5, pp. 507–521, 1996.

[7] G. Otten, T.J.A. de Vries, J. van Amerongen, A.M. Rankers, and E.W. Gaal, "Linear Motor Motion Control Using a Learning Feedforward Controller," *IEEE/ASME Transactions on Mechatronics*, vol. 2, no. 3, pp. 179–187, 1997.

[8] P. Van den Braembussche, J. Swevers, and H. Van Brussel, "Linear Motor Ripple Compensation Using Position-triggered Repetitive Control," in *Proceedings of the IFAC Workshop on Motion Control*, Grenoble, France, 1998, pp. 353–357.

[9] E. Schrijver and J. van Dijk, "H_∞ Design of Disturbance Compensators for Cogging Forces in a Linear Permanent Magnet Motor," *Journal A*, vol. 40, no. 4, pp. 36–41, 1999.

[10] F.J. Lin, C.H. Lin, and C.M. Hong, "Robust Control of Linear Synchronous Motor Servodrive Using Disturbance Observer and Recurrent Neural Network Compensator," *IEE Proceedings Electric Power Applications*, vol. 147, no. 4, pp. 263–272, 2000.

[11] T.H. Lee, K.K. Tan, S.Y. Lim, and H.F. Dou, "Iterative Learning of Permanent Magnet Linear Motor with Relay Automatic Tuning," *Mechatronic*, vol. 10, no. 1-2, pp. 169–190, 2000.

[12] L. Xu and B. Yao, "Adaptive Robust Precision Motion Control of Linear Motors with Ripple Force Compensations: Theory and Experiments," in *Proceedings of the IEEE Conference on Control Applications*, Sept. 2000, pp. 373–378.

[13] Custom Servo Motors, *Inbetriebnahmeanleitung Baureihe TBF-I und TBF-T*, 1997.

[14] Anorad Inc., USA, *Linear Motor Reference Manual*, 1999.

[15] B. Amstrong-Hélouvry, P. Dupont, and C. Canudas de Wit, "A Survey of Models, Analysis Tools and Compensation Methods for the Control of Machines with Friction," *Automatica*, vol. 30, no. 7, pp. 1083–1138, 1994.

[16] F. Altpeter, *Friction Modeling, Identification and Compensation*, Ph.D. thesis, École Polytechnique Fédérale de Lausanne, 1999.

[17] U. Brahms, *Regelung von Lineardirektantrieben für Werkzeugmaschinen*, Ph.D. thesis, Universität Hannover, 1998, VDI-Verlag, Reihe 8, Nr. 735.

[18] The Mathworks Inc., *Optimization Toolbox User's Guide*, 1999.